Int j simul model 21 (2022) 4, 555-566
Original scientific paper

SHEAR LAG EFFECT STUDY OF A COMPOSITE GIRDER CABLE-STAYED BRIDGE DURING CONSTRUCTION

She, Q. C.[*,**]; Chen, C. S.[*,#]; Yan, D. H.[*]; Wu, L. M.[**] & Huang, G.[*]
[*] School of Civil Engineering, Changsha University of Science and Technology, 410114, Changsha, China
[**] College of Civil Engineering and Architecture, Hunan Institute of Science and Technology, 414006, Yueyang, China
E-Mail: changsongchen@csust.edu.cn ([#] Corresponding author)

Abstract
To investigate the shear-lag effect in the main girder of a composite twin-box girder cable-stayed bridge during construction, a full-bridge model and a local spatial model were established using the finite element software MIDAS/Civil and ABAQUS, respectively, for the main span of the Chibi Yangtze River Bridge in Hubei Province, China, as an engineering example. On this basis, the shear-lag effect in the composite twin-box girder under multiple typical construction conditions was analysed through numerical simulation, and the accuracy of the model was verified by field measurements at the construction site. Results demonstrate that as the balanced cantilever construction progresses, the stress in the deck slabs near the junction of the anchor plate and the outer web of the side box girder and at the location of small longitudinal beams changes substantially. However, the stress at other girder sections is gradually uniformly distributed, the shear-lag coefficient tends to be stable, and a phenomenon of positive and negative shear-lag effect conversion occurs in the deck slab sections of the main girder.
(Received in June 2022, accepted in October 2022. This paper was with the authors 2 months for 2 revisions.)

Key Words: Composite Twin-Box Girder, Construction Stage, Shear-Lag Effect, Stress Test, Finite Element Method

1. INTRODUCTION

Steel-concrete composite girders are widely used as the main form of girder structure in long-span cable-stayed bridges because of their advantages of a light weight, a high stiffness, an excellent wind and seismic resistance, and the high durability of the deck pavement. However, during the construction of the balanced cantilever, the main girder of the composite girder cable-stayed bridge is subjected to a combination of loads, including the self-weight of the main girder and the anchoring force of the stay cables, causing the main girder to be in a state of compression and bending. As the anchoring force of the composite girder cable-stayed bridge is transferred from the anchor plate to steel longitudinal beams, transverse beams and small longitudinal beams and then to concrete deck slabs through shear connectors on the respective flange plates, the longitudinal stress of the concrete deck is concentrated within a limited width of the deck connected with steel longitudinal beams, transverse beams, and small longitudinal beams, thereby resulting in the nonuniform distribution of the longitudinal stress of the concrete deck slab in the transverse direction and thereby causing the shear-lag effect and concrete deck slab cracking [1].

To address these problems, numerous studies have been conducted on the influence of the shear-lag effect in composite girder bridges of different structural forms on bridge structures during their design, construction, and completion [2-7]. However, during construction, the main girders of composite girder cable-stayed bridges undergo multiple system transformations, hence resulting in a complex stress state of the main girders. In addition, during balanced cantilever construction, bridges are still unstable structural systems, and the internal forces and deformations of the main girders are more sensitive to the shear-lag effect. Therefore, the shear-lag effect in composite girder cable-stayed bridges needs to be understood accurately during

construction, and the relationship between the design position of the main steel girders and the stress distribution of the concrete deck slabs needs to be clarified.

Based on the above analysis, this study built a full model and a local spatial model of a composite girder cable-stayed bridge by combining the finite element (FE) and field measurement methods to analyse the shear-lag effect in the composite twin-box girder under multiple typical construction conditions through numerical simulation and comparison with field measurements, aiming to understand the shear-lag effect during construction more precisely to provide a reference for the design and construction of composite girder cable-stayed bridges.

2. STATE OF THE ART

In the past two decades, numerous tests and analyses have been carried out to study the shear-lag effect in composite girders. Dezi et al. [8] proposed a shear-lag displacement mode function in their model to consider the shear-lag effect in twin-I steel composite girders under static force, support settlement, and concrete shrinkage. Amadio et al. [9] experimentally and numerically evaluated the correctness and applicability of the effective width formulation suggested by Eurocode 4 [10]. Sun and Bursi [11] proposed a displacement-based two-field mixed beam element to analyse composite girders considering the shear-lag and slip effects in them, but this approach is not applicable to nonlinear structural analysis. To solve for the spatial variables, Gara et al. [12-14] incorporated four displacement functions (i.e., the longitudinal and vertical displacements of the concrete slab and steel beam) and the strength function of the entire beam into the virtual work equation and analysed the shear-lag and slip effects of the composite beam by solving the equations numerically using the FE method. However, numerical errors, albeit small, are common when using the FE method because of spatial discretization. In view of the use of the effective width in the design calculation of composite girder bridges, Zhu et al. [15] proposed a simplified analysis method based on the effective width to consider the shear-lag effect in composite girder bridges, hence facilitating design and analysis. Based on the energy variational principle, Chen et al. [16] established analytical equations for calculating the shear-lag coefficients of composite box girders with corrugated steel webs and trusses, verified their validity using the results of segmented model tests and FE methods, and investigated the influence of various factors on the shear-lag effect in this type of structure. In response to the fact that concrete in continuous composite girder bridges is significantly influenced by cracking, creep, and shrinkage effects, Varshney et al. [17] proposed an effective and novel strategy of using fibre-reinforced concrete near the internal supports of continuous beams, which can reduce cracking greatly according to the results of numerical investigations. Masoudnia [18] reviewed the relevant literature on the analysis of the shear-lag effect in steel-concrete composite beams and pointed out that although many studies have been conducted on the influence of different structural parameters on the effective flange width, some design details still need to be considered carefully. Zhang et al. [19] investigated the shear-lag effect in the negative moment region of the concrete slab in steel-concrete composite beams under cyclic fatigue loads through large-scale tests and numerical simulation analysis and explored the transverse reinforcement stress distribution in the negative moment region of steel-concrete composite beams, as well as the influence of design parameters (e.g., concrete slab thickness and shear connector stiffness) on the effective flange width. To clarify the shear-lag effect in the cross-section of steel bottom-corrugated steel web box girders, Gong et al. [20] investigated the influence of replacing the concrete floor slab with a steel bottom on the additional warping displacement of the steel-concrete cross-section based on the energy variational principle of the cosine function method. Based on the principle of virtual work, Huang et al. [21, 22] analysed the influence of the time-varying characteristics of the contact

section of old and new concrete on the shear-lag effect in composite beams and reasonably predicted the long-term performance of composite beams, which helps in the life-cycle design and service performance analysis of composite bridges. Sampayo et al. [23] analysed the chassis design using finite element analysis and multibody dynamic simulation.

The above results are mainly related to the shear-lag effect obtained in experimental research, theoretical analyses, and numerical investigations of segmented models of composite girders. Research on the shear-lag effect in composite girder cable-stayed bridges is limited, especially research related to the shear-lag effect in the construction stage. To understand the stress state of the main girder deck slabs of composite twin-box girder cable-stayed bridges and to ensure the safety and reliability of the main girder during construction, this study used the main girder of the Chibi Yangtze River Bridge in Hubei Province, China, as an engineering example to field test the deck slab stress under several typical construction conditions during the balanced cantilever construction of the main girder of the bridge. With full consideration of the influence of steel longitudinal beams, transverse beams, and small longitudinal beams on the shear-lag effect in the concrete deck slab, full-bridge and local FE models were established using MIDAS/Civil and ABAQUS software, respectively, to conduct a refined analysis of the stress state of the deck slabs of the composite twin-box girder cable-stayed bridge during the balanced cantilever construction stage, thereby providing a basis for the design and construction of composite twin-box girder cable-stayed bridges.

The remainder of this study is organized as follows. Section 3 builds the models used for full-bridge and local calculations. Section 4 presents the FE analysis of the construction process of the main girder of the Chibi Yangtze River Bridge, verifies the accuracy of the FE models by field measurements, and analyses the shear-lag effect in the bridge deck during construction comparatively through numerical simulation. Section 5 summarizes the conclusions.

3. METHODOLOGY

3.1 Full-bridge modelling with MIDAS

An overall model of the full bridge is built using MIDAS CIVIL. The main bridge is reasonably discretized into a spatial bar-system structure according to factors, such as construction stages (Fig. 1). Specifically, the full bridge is discretized into 1984 elements with 2239 nodes, considering a total of 177 construction stages. The stay cables are modelled using truss elements, and all other members are modelled using beam elements. There are 372 elements for the main pylons, auxiliary piers, and side piers, 1370 elements for the main girder, and 232 elements for the stay cables. The connections between the cables and the main pylons and between the cables and the anchor plates of the main girder are simulated by rigid connections in the elastic connections of the software, the connections between the main steel girder and the anchor plates are simulated by two-node rigid connections in the software, and the wet joints and precast bridge deck are simulated as a single element. The alignment of the cable tower and the main girder is established according to the design alignment. A layer of elements is established for the main steel girder and deck slab, between which the connection is simulated by a two-node rigid connection in the software. The entire construction of the full bridge is modelled to obtain accurate results for the displacement, stress, and internal force at each bridge construction stage and in the completed bridge.

To simplify the model, the following approximations are made in the actual modelling:

(1) Except for the cable sag effect, the nonlinearity effect of the main girder and pylons is not considered.

(2) The slip effect of the main steel girder and concrete deck slab is ignored.

(3) The modulus of the cables is corrected using Ernst's formula, considering the nonlinearity effect of the flexible cables.

(4) The material nonlinearity effect is ignored, and linear elastic materials are used to model the main steel girder, cables, and concrete.

By performing an overall analysis of the bridge for the entire construction process, the normal stresses of the concrete deck slab along the bridge longitudinal direction under each construction condition, that is, the stresses based on the elementary beam theory, are obtained for the subsequent shear-lag effect analysis.

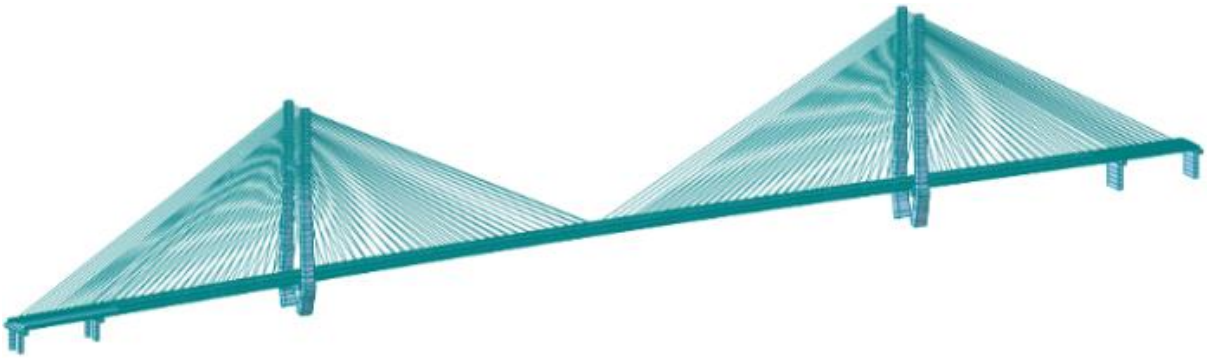

Figure 1: Overall model of the full bridge.

3.2 Local modelling with ABAQUS

The key issues regarding the element selection, meshing, boundary conditions, and interfaces in the FE modelling with ABAQUS are briefly described as follows.

Element selection and meshing: The concrete deck slab and anchor plates were modelled using three-dimensional eight-node solid elements with reduced integration scheme (C3D8R). The main steel girder (consisting of longitudinal beams, transverse beams, and small longitudinal beams) was modelled using four-node shell elements with reduced integration scheme (S4R), employing nine Simpson's integration points over the thickness of the shell element to meet the calculation accuracy requirement. The structured meshing technique was adopted, and the consistency of the meshes at the contact surfaces was maintained.

Cross-section modelling: The longitudinal beams, transverse beams, and small longitudinal beams were modelled separately and then combined directly into a main steel girder using the "merge" function. The slip effects between the concrete deck slab and the main steel girder, as well as between the anchor plates and the longitudinal beams, were ignored, and their contact surfaces were realized using the "Tie" function. The intersection of the anchor plates and the concrete deck slab was modelled using the "Embedded region" function, where the anchor plates were the embedded region in the concrete deck slab, and the concrete deck slab was in the main region.

Boundary conditions and loads: During the construction of the three segments at the top of the main girder pier, three-directional (longitudinal, transverse, and vertical) temporary fixity was used for the main girder and the main pylon to ensure the stability and safety of the structure throughout the construction process. Therefore, to obtain results consistent with the actual working conditions of the project, only the 1/2 middle span of the bridge was modelled, and the fixity boundary condition was employed for the main girder in the pylon region. The loads mainly included the self-weight of the structure, the forces of the stay cables, and the self-weight of the crane. In particular, the cable forces were extracted from the MIDAS full-bridge model according to the calculation conditions of the corresponding construction stage and applied to the anchor plates as concentrated forces.

In this study, the simulation was performed in the ABAQUS/Standard module. The structural stresses in any working condition and at any location of the main girder could be obtained from local analysis for subsequent analysis. The local spatial model is shown in Fig. 2.

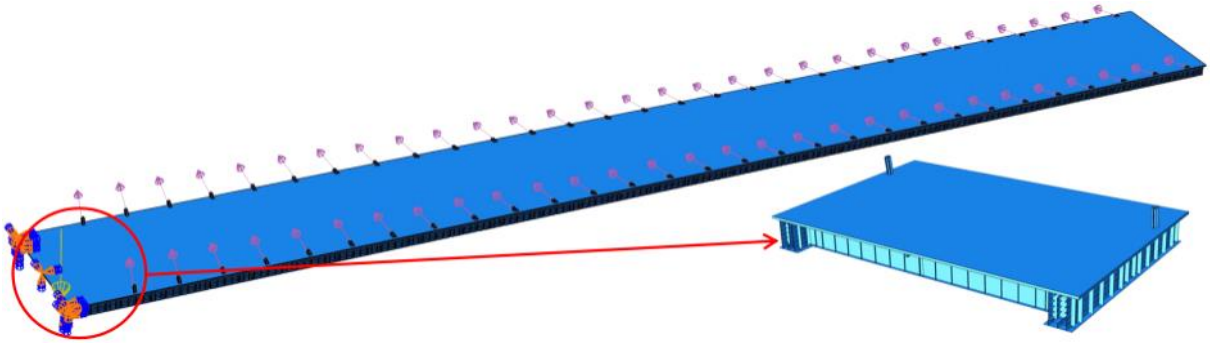

Figure 2: Local spatial FE model (in the maximum balanced cantilever construction stage).

3.3 Stress acquisition method

The stress of the concrete deck slab were collected in the field by a comprehensive tester and embedded intelligent string strain gauges JMZX-215 HA. The test using strain gauges provided an understanding of the strain (i.e., deformation) on the concrete deck slab, and the stresses were calculated using the elastic modulus of the concrete. In general, the initial values of the strain gauges were read after they were installed, and the structure was stabilized, and the measured strain values were then read when forces were applied to the structure (or in other situations). The strain values of the structure were calculated by subtracting the initial values from the measured values and then multiplying by the concrete elastic modulus to obtain the stress values. The strain gauges had the following technical parameters: sensitivity, 1 με; accuracy, 0.1 % *FS*; range, ±1500 με; and gauge length, 146 mm.

4. RESULT ANALYSIS AND DISCUSSION

4.1 Bridge overview

The main bridge of the Chibi Yangtze River Bridge is a steel-concrete composite girder cable-stayed bridge with double pylons and double cable planes. Its elevation is shown in Fig. 3 a. The main bridge has a span arrangement of (90+240+720+240+90) m, with the main span of 720 m being the longest in the world among bridges of this type. The deck is 36.5 m wide, and its cross-section is shown in Fig. 3 b.

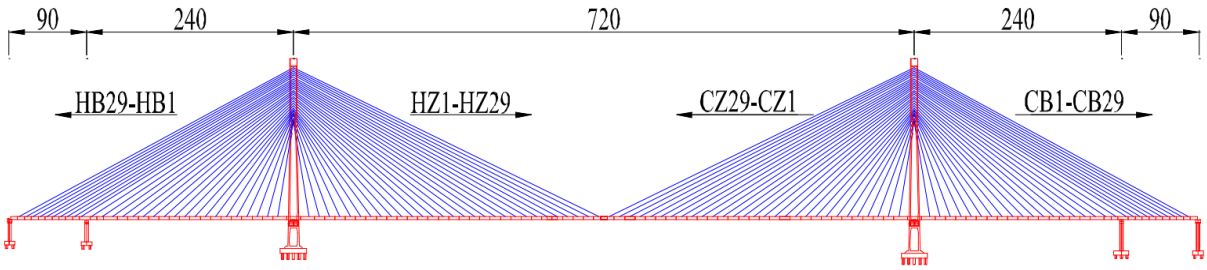

a) Elevation of the main bridge

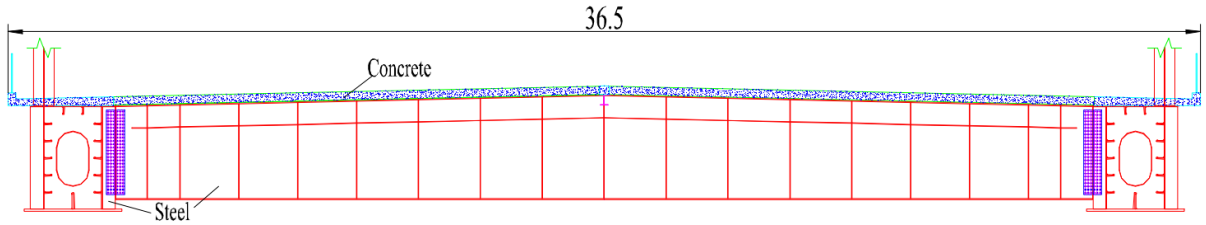

b) Standard cross-section of composite girder

Figure 3: Chibi Yangtze River Bridge (units: m).

The main girder adopts the form of a twin-box section, which consists of a steel box girder and a precast concrete deck, with thicknesses of 3.181 m and 26 cm in a standard segment, respectively, that are connected by shear connectors arranged on the longitudinal beams, transverse beams, and small longitudinal beams. The main steel girder in the standard segment is 12 m long and 35.12 m wide and consists of two side steel box girders, three steel transverse beams (with a spacing of 4 m), and a small longitudinal beam. In the standard segment, stay cables are anchored to the main girder by anchor plates, which are arranged directly above the intersection of the middle transverse beam and the outer web of the side box girder. The cables are spaced at 12 m in the middle span and 8, 12, or 16 m in the side spans. The main girder was built symmetrically using the balanced cantilever construction method. During this process, the stay cables were tensioned twice, with the first tensioning after the main steel girder was fully bolted and welded and the second tensioning after the wet joints were cured. The local schematic diagram of the main girder of the twin-box composite girder cable-stayed bridge is shown in Fig. 4. Table I lists the material properties.

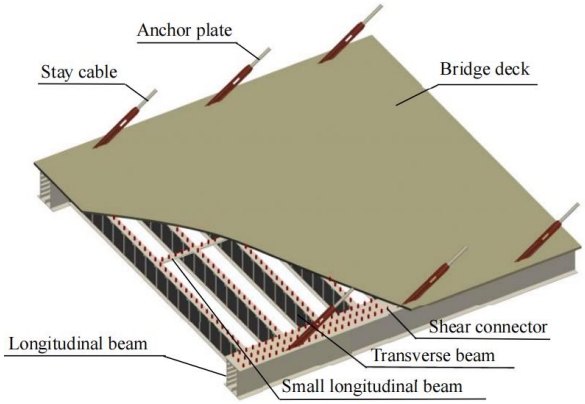

Figure 4: Local schematic diagram of the main girder of the twin-box composite girder cable-stayed bridge.

Table I: Material properties.

Structure	**Material**	**Elastic modulus** (Gpa)	**Density** (kg/m^3)
Steel girder	Q420qD	206	7850
Stay cable	PE galvanized steel	195	7850
Bridge deck, PC beam	C60	35.5	2625
Pylon	C50	34.5	2625

4.2 FE analysis

Based on the analysis using the ABAQUS FE software in Section 3.2, the stresses in the deck slab along the bridge longitudinal direction in six typical construction conditions (Table II) were obtained (Fig. 5).

Table II: Six typical construction conditions.

CC	**Description**
CC1	Completion of two tensioning operations for girder segment #1 (CZ1/CB1)
CC2	Completion of two tensioning operations for girder segment #6 (CZ6/CB6)
CC3	Completion of two tensioning operations for girder segment #16 (CZ16/CB16)
CC4	Completion of two tensioning operations for girder segment #18 (CZ18/CB18)
CC5	Completion of two tensioning operations for girder segment #24 (CZ24/CB24)
CC6	Completion of two tensioning operations for girder segment #29 (CZ29/CB29) (Maximum balanced cantilever construction stage)

Note: CC represents construction condition.

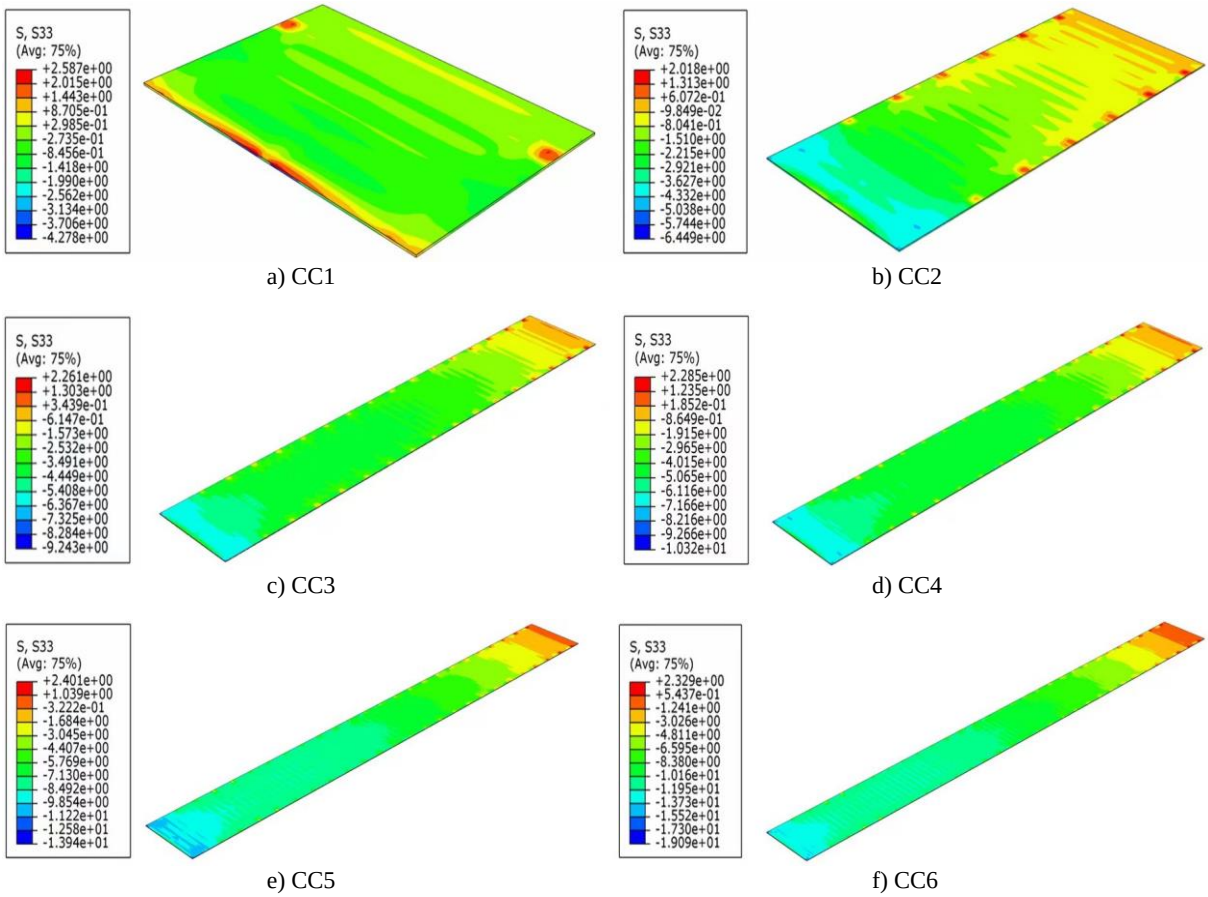

Figure 5: Stresses in the deck slab along the bridge longitudinal direction under different CC (unit: MPa).

4.3 Experimental study

To obtain the stresses in the concrete deck slab during the construction of the main bridge girder in real time, three concrete stress test sections (e.g., S1, S2, and S3) were arranged in girder segments #1, #6, and #16 of the middle span on the south side of the bridge, with distances of 14 m, 78 m and 194 m from the centreline of the pylon, respectively (Fig. 6). A total of 15 strain gauges were placed on each section. Fig. 7 shows the transverse positions of the strain gauges on the test section. Using the stress acquisition equipment in Section 3.3, the stresses at the measurement points of sections S1 to S3 were collected under CC1 to CC6 (Fig. 8).

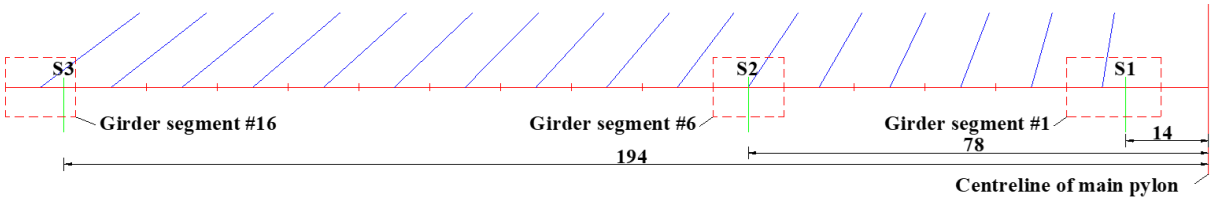

Figure 6: Test girder segments and test sections (unit: m).

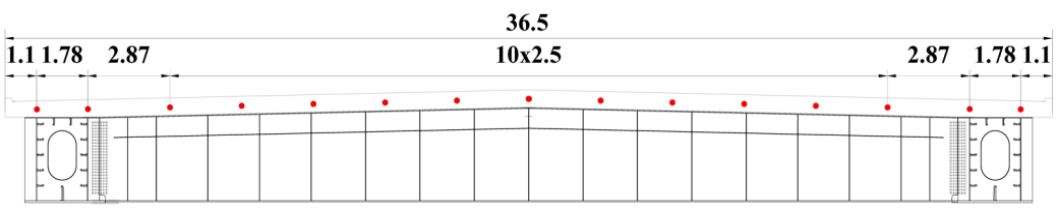

Figure 7: Transverse arrangement of strain gauges on the test section (unit: m).

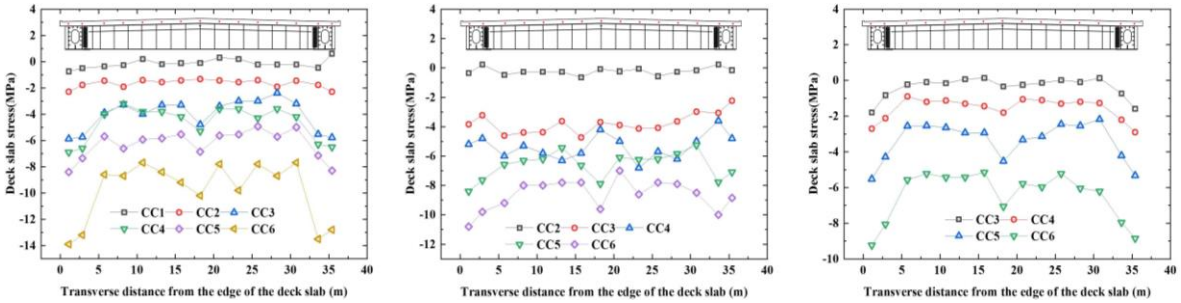

a) Section S1 b) Section S2 c) Section S3

Figure 8: Measured values of stresses on sections S1-S3.

As shown in Fig. 8, during the construction of the main girder, stresses in the deck slab were nonuniformly distributed along the transverse direction, showing a considerable shear-lag effect. Moreover, a particularly substantial phenomenon of an abrupt change in stress was observed at the location of the side box girders and small longitudinal beams.

4.4 Comparative analysis

Based on the numerical analysis and field-measured data in Sections 3.1, 3.2, and 3.3, the field-measured data and calculated values were analysed comparatively using CC6 as an example. The specific data are shown in Fig. 9.

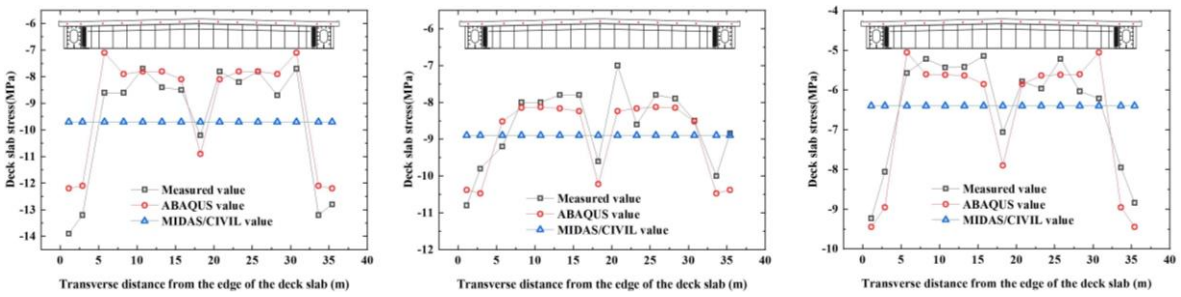

a) Section S1 b) Section S2 c) Section S3

Figure 9: Measured and calculated values of stresses on test sections (CC6).

Fig. 9 show that under CC6, a substantial shear-lag effect occurred in test sections S1 to S3, with a shear-lag coefficient ranging from 0.8–1.4. The measured and calculated values in the bridge transverse direction had consistent distribution patterns, indicating the reliability of the FE model established in this study. Therefore, the shear-lag effect in the deck slabs was further investigated using ABAQUS FE software.

4.5 Analysis of the shear-lag effect in the deck slabs

The shear-lag effect in the concrete deck slabs of the main girder was further analysed using CC6 (maximum balanced cantilever construction stage) as an example.

Analysis of the shear-lag effect in the standard segment: To fully consider the influence of the side steel box girders, transverse beams, and small longitudinal beams on the shear-lag effect in the deck slabs, six cross-sections (labelled I-I to VI-VI) with a spacing of 2 m were selected in the standard main steel girder segment (Fig. 10). Section III-III is the cable anchorage section; section VI-VI is the middle section between two stay cables; sections I-I, III-III, and V-V are connected to transverse beams; and sections II-II, IV-IV, and VI-VI are the middle sections between two adjacent transverse beams. The abovementioned stress test section S1 is section V-V in girder segment #1, section S2 is section III-III in girder segment #6, and section S3 is section V-V in girder segment #16.

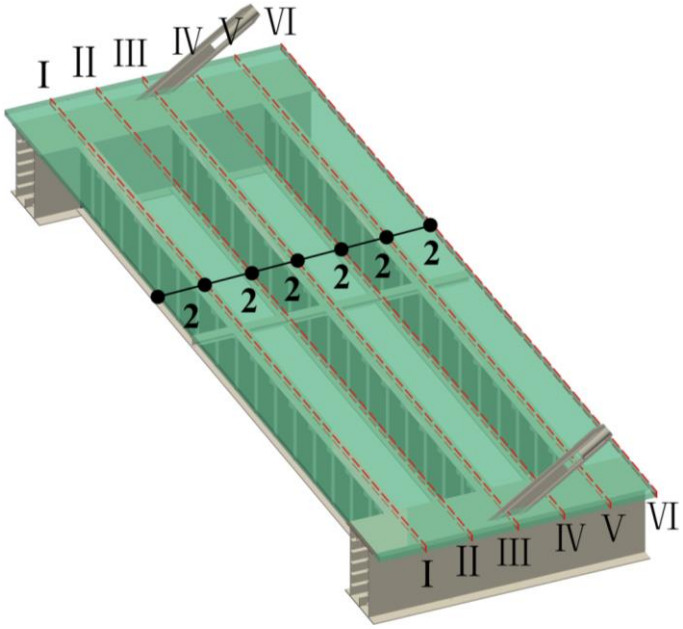

Figure 10: Schematic diagram of six sections in the bridge transverse direction in the standard segment (unit: m).

Based on the ABAQUS FE software as described in Section 3 2, the stresses at six deck slab cross-sections in girder segment #1 under CC1, #6 under CC2, #16 under CC3, and #1, #6, and #16 under CC6 were analysed, as plotted in Figs. 11 and 12.

As shown in Figs. 11 and 12, (1) after the cable tensioning, a substantial shear-lag effect was present in the deck slabs, especially a marked, abrupt change in the stress of the deck slab at the junction of the anchor plate and the outer web of the side box girder. (2) As the construction progressed, a conversion between positive and negative shear-lag effects occurred in the bridge slabs. For example, the negative shear-lag effect in the deck slab at the anchorage section (section III-III) of the previously constructed girder segment changed into a positive shear-lag effect, whereas the positive shear-lag effect in the deck slab along the middle section between the stay cables (section VI-VI) changed into a negative shear-lag effect. (3) The presence of transverse beams and their shear connectors had a large impact on the shear-lag effect in the deck slab. For example, during the maximum balanced cantilever construction stage, a substantial positive shear-lag effect occurred in the deck slabs of the sections connected to the transverse beams (sections I-I, III-III, and V-V), and a substantial negative shear-lag effect persisted in the deck slabs of the other sections not connected to the transverse beams. (4) Finally, an abrupt change in stress occurred in the deck slabs of all sections at the location of the small longitudinal beams, with the stress value close to the value from elementary beam theory, indicating that the installation of small longitudinal beams reduced the shear-lag effect to some extent.

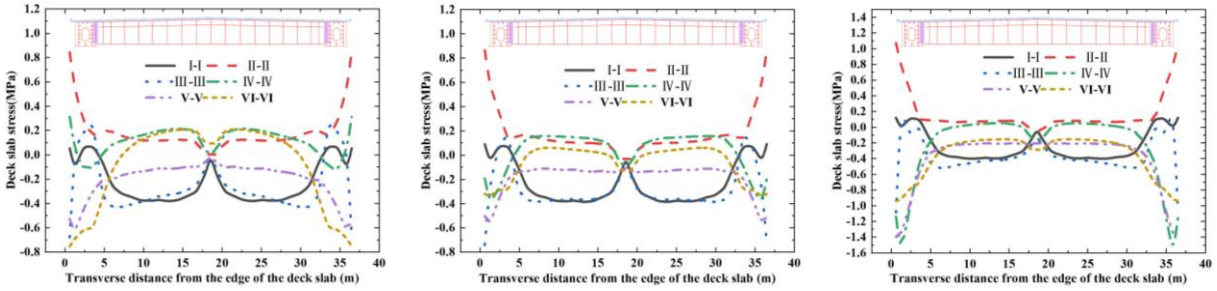

a) Girder segment #1 (under CC1) b) Girder segment #6 (under CC2) c) Girder segment #16 (under CC3)

Figure 11: Deck slab stress values at different cross-sections of girder segments.

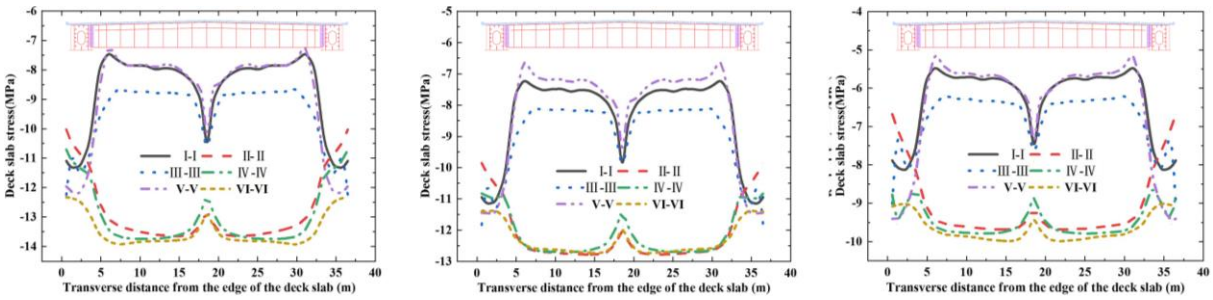

a) Girder segment #1 b) Girder segment #6 c) Girder segment #16

Figure 12: Deck slab stress values at different cross-sections of girder segments (under CC6).

Shear-lag coefficient of the deck slab: The shear-lag coefficient is obtained as the ratio of the value calculated by the ABAQUS simulation analysis considering the shear-lag effect to the value calculated by the MIDAS simulation analysis according to elementary beam theory. The shear-lag coefficients of the cable anchorage section (section III-III) and the middle section between stay cables (section VI-VI) under CC6 are shown in Fig. 13, where *X* is the distance from the corresponding section to the centreline of the bridge pylon.

Fig. 13 shows that during the maximum balanced cantilever construction stage, a considerable positive shear-lag effect occurred in the anchorage section, and a substantial negative shear-lag effect occurred in the middle section between stay cables. With the progress of the construction stage, the shear-lag coefficient tended to be stable in the sections of previously completed girder segments, except for sections with large changes in stress (i.e., deck slabs near the junction of the anchor plate and the outer web and at the position of small longitudinal beams).

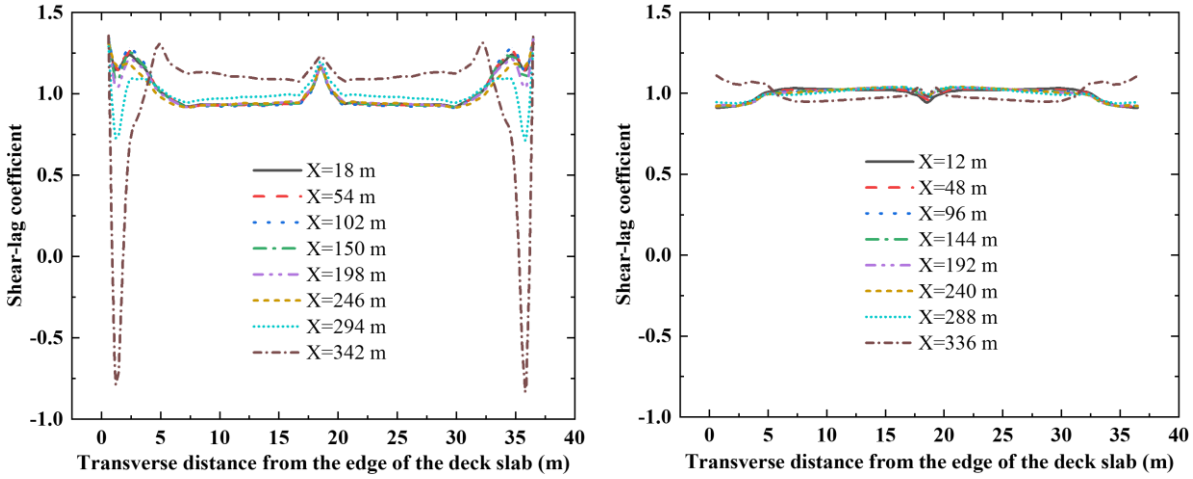

a) Anchorage section b) Middle section between stay cables

Figure 13: Shear-lag coefficient of each cross-section deck (under CC6, *X* denotes the distance between the test section and the centreline of the pylon).

5. CONCLUSION

To investigate the shear-lag effect in the main girder of the composite twin-box girder cable-stayed bridges during construction and to reveal the stress state of the concrete deck slab as the construction stage advances, this study analysed the shear-lag effect during the construction of the main bridge of the Chibi Yangtze River Bridge using field bridge test and FE numerical analysis and investigated the variation pattern of the shear-lag effect in the concrete deck slab. The following conclusions could be drawn as follows:

(1) During the balanced cantilever assembly of the main girder, the stress in the concrete deck slab is distributed nonuniformly in the transverse direction and mainly concentrated in an effective width range near the side steel box girders, transverse beams, and small longitudinal beams, thereby showing a substantial shear-lag effect.

(2) A remarkable phenomenon of abrupt changes occurred in the stress of the deck slab at the junction of the anchor plate and the outer web of the side steel box girder. In design, the thickness of the flange plate and web can be increased appropriately or stiffeners can be added to ensure safety under load. Moreover, a significant phenomenon of abrupt changes in the stress of the deck slab occurred at the location of small longitudinal beams with the stress values close to those calculated by elementary beam theory, indicating that the installation of small longitudinal beams reduced the shear-lag effect to some extent. The influence of small longitudinal beams can be ignored in design calculations to generate results that err on the side of caution.

(3) With the progress of construction, except for the large stress changes in the deck slab of the girder segment sections near the junction of the anchor plate and the outer web and at the location of the small longitudinal beams, the closer the girder segment was to the pylon area, the more uniform the stress distribution in the deck slab became; that is, the shear-lag coefficient tended to be stable, and a phenomenon of conversion between positive and negative shear-lag effects occurred between the anchorage section of the deck slab and the middle section between the stay cables.

In this study, the shear-lag effect in bridge deck slabs during construction was analysed by combining the field bridge test and FE numerical analysis, and the obtained variation pattern of the shear-lag effect in concrete deck slabs provides a reference for the future design and construction of composite girder cable-stayed bridges. The presented variation pattern is only suitable for the middle span of the main girder because of the lack of field-measured stress data for the side span of the main girder. Therefore, in future research, the field-measured data for the side span of the main girder will be used to modify the model so that the variation pattern of the shear-lag effect of the concrete deck slab of the full bridge will be understood more accurately.

ACKNOWLEDGEMENT

This study was supported by the National Natural Science Foundation of China (Grant No. 51878073, No. 52278143 and No. 52278141) and the Research Foundation of Education Department of Hunan Province (Grant No. 19A208). The authors express their great appreciation and sincere gratitude.

REFERENCES

[1] Wang, Y.; Shao, X. D.; Cao, J. H. (2019). Experimental study on basic performances of reinforced UHPC bridge deck with coarse aggregates, *Journal of Bridge Engineering*, Vol. 24, No. 12, Paper 04019119, doi:10.1061/(ASCE)BE.1943-5592.0001492

[2] Hu, S. W.; Yu, J.; Wei, C. J.; Zhang, Z. G. (2017). Shear lag behavior and parametric sensitivity analysis of steel-concrete composite structure with double-box, *Archive of Applied Mechanics*, Vol. 87, No. 9, 1525-1539, doi:10.1007/s00419-017-1268-3

[3] Zhu, L.; Nie, J. G.; Ji, W. Y. (2017). Positive and negative shear lag behaviors of composite twin-girder decks with varying cross-section, *Science China Technological Sciences*, Vol. 60, No. 1, 116-132, doi:10.1007/s11431-016-0314-x

[4] Tong, T.; Yu, Q.; Su, Q. T. (2018). Coupled effects of concrete shrinkage, creep, and cracking on the performance of postconnected prestressed steel-concrete composite girders, *Journal of Bridge Engineering*, Vol. 23, No. 3, Paper 04017145, doi:10.1061/(ASCE)BE.1943-5592.0001192

[5] Szurgott, P.; Bernacki, P. (2020). Modelling of steel-concrete bridges subjected to a moving high-speed train, *International Journal of Simulation Modelling*, Vol. 19, No. 1, 29-40, doi:10.2507/IJSIMM19-1-499
[6] Lezgy-Nazargah, M.; Vidal, P.; Polit, O. (2019). A sinus shear deformation model for static analysis of composite steel-concrete beams and twin-girder decks including shear lag and interfacial slip effects, *Thin-Walled Structures*, Vol. 134, 61-70, doi:10.1016/j.tws.2018.10.001
[7] Wang, G.-M.; Zhu, L.; Zhou, G.-P.; Han, B.; Ji, W.-Y. (2020). Experimental research of the time-dependent effects of steel-concrete composite girder bridges during construction and operation periods, *Materials*, Vol. 13, No. 9, Paper 2123, 18 pages, doi:10.3390/ma13092123
[8] Dezi, L.; Gara, F.; Leoni, G. (2003). Shear-lag effect in twin-girder composite decks, *Steel and Composite Structures*, Vol. 3, No. 2, 111-122, doi:10.12989/scs.2003.3.2.111
[9] Amadio, C.; Fedrigo, C.; Fragiacomo, M.; Macorini, L. (2004). Experimental evaluation of effective width in steel-concrete composite beams, *Journal of Constructional Steel Research*, Vol. 60, No. 2, 199-220, doi:10.1016/j.jcsr.2003.08.007
[10] EN 1994-2 (1997). *Eurocode 4 – Design of composite steel and concrete structures – Part 2: General rules and rules for bridges*, European Committee for Standardization, Brussels
[11] Sun, F.-F.; Bursi, O. S. (2005). Displacement-based and two-field mixed variational formulations for composite beams with shear lag, *Journal of Engineering Mechanics*, Vol. 131, No. 2, 199-210, doi:10.1061/(ASCE)0733-9399(2005)131:2(199)
[12] Gara, F.; Ranzi, G.; Leoni, G. (2008). Analysis of the shear lag effect in composite bridges with complex static schemes by means of a deck finite element, *International Journal of Steel Structures*, Vol. 8, No. 4, 249-260
[13] Gara, F.; Leoni, G.; Dezi, L. (2009). A beam finite element including shear lag effect for the time-dependent analysis of steel-concrete composite decks, *Engineering Structures*, Vol. 31, No. 8, 1888-1902, doi:10.1016/j.engstruct.2009.03.017
[14] Gara, F.; Ranzi, G.; Leoni, G. (2010). Short- and long-term analytical solutions for composite beams with partial interaction and shear-lag effects, *International Journal of Steel Structures*, Vol. 10, No. 4, 359-372, doi:10.1007/bf03215844
[15] Zhu, L.; Nie, J.-G.; Li, F.-X.; Ji, W.-Y. (2015). Simplified analysis method accounting for shear-lag effect of steel-concrete composite decks, *Journal of Constructional Steel Research*, Vol. 115, 62-80, doi:10.1016/j.jcsr.2015.08.020
[16] Chen, Y. Y.; Dong, J. C.; Xu, T. H.; Xiao, Y. F.; Jiang, R. J.; Nie, X. M. (2019). The shear-lag effect of composite box girder bridges with corrugated steel webs and trusses, *Engineering Structures*, Vol. 181, 617-628, doi:10.1016/j.engstruct.2018.12.048
[17] Varshney, L. K.; Patel, K. A.; Chaudhary, S.; Nagpal, A. K. (2019). An efficient and novel strategy for control of cracking, creep and shrinkage effects in steel-concrete composite beams, *Structural Engineering and Mechanic*s, Vol. 70, No. 6, 751-763, doi:10.12989/sem.2019.70.6.751
[18] Masoudnia, R. (2020). State of the art of the effective flange width for composite T-beams, *Construction and Building Materials*, Vol. 244, Paper 118303, 18 pages, doi:10.1016/j.conbuildmat.2020.118303
[19] Zhang, J. Q.; Han, B.; Xie, H. B.; Yan, W. T.; Li, W. W.; Yu, J. P. (2021). Analysis of shear lag effect in the negative moment region of steel-concrete composite beams under fatigue load, *Steel and Composite Structures*, Vol. 39, No. 4, 435-451, doi:10.12989/scs.2021.39.4.435
[20] Gong, B. J.; Liu, S. Z.; Mao, Y. N.; Qin, A. A.; Cai, M. H. (2022). Correction of shear lag warping function of steel bottom – corrugated steel web box girder, *Structures*, Vol. 37, 227-241, doi:10.1016/j.istruc.2021.12.084
[21] Huang, D. W.; Wei, J.; Peng, H.; Guo, H. L.; Wang, B. W. (2022). An analysis model accounting for time-dependent shear lag effects in assembled composite bridge decks, *Advances in Structural Engineering*, Vol. 25, No. 9, 1866-1877, doi:10.1177/13694332221080601
[22] Huang, D. W.; Wei, J.; Liu, X. C.; Xiang, P.; Zhang, S. Z. (2019). Experimental study on long-term performance of steel-concrete composite bridge with an assembled concrete deck, *Construction and Building Materials*, Vol. 214, 606-618, doi:10.1016/j.conbuildmat.2019.04.167
[23] Sampayo, D.; Luque, P.; Mantaras, D. A.; Rodriguez, E. (2021). Go-kart chassis design using finite element analysis and multibody dynamic simulation, *International Journal of Simulation Modelling*, Vol. 20, No. 2, 267-278, doi:10.2507/IJSIMM20-2-555